Electronic Supporting Information

Leveraging Metal Oxide-Fenugreek Hydrogel Nanocomposites for Enhanced Structural and Biological Properties

Debolina Ghosh[a], Deepmoni Deka[a] Gopal Das[a,b]*

[a] Centre for the Environment, Indian Institute of Technology Guwahati, Assam 781039, India,

[b] Department of Chemistry, Indian Institute of Technology Guwahati, Assam 781039, India,

E-mail: gdas@iitg.ac.in

Experimental Section

1. Materials

Fenugreek seeds were purchased locally. Ethanol, Glycerol, and the other reagents for phytochemical analysis were purchased from SRL, India. $FeCl_3$, $CuSO_4$, and $KMnO_4$ salts were purchased from Sigma Aldrich. All the chemicals were of analytical grade and used in the experiments without further purification.

2. General Information

The UV-Visible absorption spectra were archived on a Perkin-Elmer Lamda-750 UV-Vis spectrophotometer using 10 mm path length quartz cuvettes in 200-800 nm wavelengths. Baseline correction was applied for all spectra.

FT-IR Spectroscopy

The prepared hydrogels were freeze-dried overnight in a lyophilizer (Labconco Freeze Dryer) and then finely grounded into a powder for Fourier transform infrared spectroscopy (FT-IR) analysis that was recorded at a resolution of 4 cm^{-1} in the scanning range 400–4000 cm^{-1} with a PerkinElmer (Spectrum 1) spectrophotometer.

Thin Film XRD

Rigaku Smartlab X-ray diffractometer (model TTRAX III) was employed for thin film X-ray diffraction (XRD) measurements at 50 kV, 100 mA using Cu-Kα (λ = 1.5406 Å) radiation for the analysis of hydrogel samples in the diffraction angle (2θ) range of 5–80° at a scanning rate of 0.02° s^{-1}. The originally prepared hydrogel film samples (200ul) were drop cast into a coverslip and allowed to dry in a hot air oven at 40°C for 4 hours, before sample analysis.

Rheology

The rheological studies were carried out on Interfacial Rheometer (model: Physica MCR 301, make: Anton Paar (Austria)) by using a 50 mm diameter at 1° angle parallel-plate geometry at 25 °C with 0.1 mm gap. The amplitude and frequency sweep tests were performed to determine the viscoelastic nature of hydrogels. The flow behavior of hydrogels was analyzed by the Power Law model as per literature given as

$$\eta = m(\dot{\gamma})\, n^{-1}$$

where η is the apparent viscosity, $\dot{\gamma}$ is the shear rate, n is the power-law index, and m is the consistency index. Amplitude sweep measurement was performed within a strain range of 0.1 to 100% at a constant 0.1 Hz frequency and in a frequency range of 0.1 to 100 Hz, with a 0.1 % strain which was considerably below the hydrogel's deformation range. Furthermore, loss tangent (tanδ), the ratio of viscous to elastic nature of hydrogel, is given by,

$$\tan\delta = G''/G'$$

where G' is the storage modulus and G" is the loss modulus. [1]

Surface morphology

The surface morphological characterization of the nanoparticles and synthesized hydrogels was performed by FESEM (model: Gemini SEM 300, make: Carl Zeiss). The freeze-dried hydrogel samples were deposited on the given sample stub using carbon tape, and subsequently, the stub was sputter-coated with a double layering of gold. FESEM image was recorded at 5-micron optical zoom, at a potential of 5.00 kV.

Thermogravimetric Analyses

The thermogravimetric profile of the nanoparticles and dried hydrogel samples was performed under a nitrogen atmosphere at a heating rate of 10 °C min^{-1} in a temperature region of 25-650 °C by employing a Netzsch STA-409CD thermal analyzer.

Swelling Studies

A known weight of dried hydrogel samples was immersed in DI water and its original pH, allowed to swell and reach the equilibrium condition. After overnight incubation, the now swollen hydrogel samples were taken out, filtered, and weighed again. The swelling ratio was obtained as follows,

$$\text{Swelling Ratio \%} = \frac{Wf - Wi}{Wi} x100$$

Where W_i = Initial weight of the hydrogel and W_f = Final weight of the hydrogel.

3. Determination of DPPH (Radical Scavenging Assay)

Radical scavenging activity of the hydrogels was determined essentially as described by Blois (1958). The concentration of hydrogels varied from 5-25 mg/ml). The volume was adjusted to 100 µl by adding MeOH. 5.0 ml of 0.1 mM methanolic solution of DPPH was added to these tubes and shaken vigorously. The tubes were allowed to stand at 25 °C for 30 min. The control

was prepared as above without any extract and MeOH was used for the baseline correction. The changes in the absorbance of the samples were measured at 517 nm. Radical scavenging activity was expressed as the inhibition percentage and was calculated using the following formula, [2]

$$\frac{C\ O.D\ -\ S\ O.D}{C\ O.D} x100$$

Where C is the control and S is the sample undergoing analysis.

4. Antibacterial Studies

The antibacterial performance of the nanocomposite hydrogels was evaluated against gram-positive (*B. subtilis* MTCC 441) and gram-negative (*E.coli* DH5α MTCC 433) strains by zone inhibition and Growth curve tests.

4.1. Growth Curve Test:

From an overnight grown fresh culture, 1% inoculum of gram-negative *E. coli* and gram-positive *B. subtilis* culture was given in Luria Bertani broth medium in each of 4 flasks. One was kept as control, with only the respective bacterial cultures, another flask had only Fenu hydrogel (25 mg/ml), and other flasks had sonicated nanocomposite hydrogel film samples (25mg/ml). The flasks were incubated at 37 ° C 180 rpm, and periodic samples were withdrawn for O.D measurement at 600 nm in a UV-Spectrophotometer.

4.2. Evaluation of Zone of Inhibition by Well-Diffusion Method

The antibacterial property of the nanocomposite hydrogels was further ascertained by the determination of the zone of inhibition by the well-diffusion method. Firstly, the respective bacterial lawn was prepared in sterile nutrient agar media plates using sterile cotton swab sticks. 10^6 CFU/ml cultures of freshly overnight-grown bacterial suspensions of *E.coli* and *B.subtilis* were used to prepare the lawn culture on the plates. Following this, wells of approximately 5mm in diameter were made, and 100µl of (25mg/ml) sonicated hydrogel film samples were added to the wells. The plates were then kept for incubation at 37°C, overnight.[3]

4.3. FESEM imaging of treated and untreated Bacterial Cells

E. coli and *B. subtilis* bacterial cells were grown in fresh LB broth (1%), overnight. After this, a known concentration of bacterial cells (O.D count: 0.2), were exposed to 1 mg/ml Fenu, CuO,

MnO_2, and Fe_2O_3 hydrogel samples, with the untreated cells as control. The cells were kept for incubation at 37°C, overnight. Subsequently, the treated as well as control bacterial cell samples (untreated) were washed thrice with sterile PBS to remove unwanted media and finally with sterile MilliQ grade water. The samples were then fixed with 4% glutaraldehyde and then gradually dehydrated with (50-100%) ethanol. The samples were finally air-dried in a laminar hood and examined in a field emission scanning electron microscope (Zeiss Gemini, USA), and their images were recorded.[4]

4.4 DNA Fragmentation Studies

E. coli cells (DH5α) harboring pET28a plasmids were grown in LB broth containing kanamycin. The cells were grown for 5 hours followed by the extraction of the plasmid from the bacteria following standard protocols.[5] The plasmid concentration was then analyzed using a NanoDrop, whereby the concentration was found to be 220ng/µl. For each reaction setup, 2.5 µl of plasmid (i.e. 550 ng of DNA was loaded onto the agarose gel). The agarose gel was prepared by dissolving 0.7 g of agarose in 1X TAE Buffer (100 ml). The gel was stained with EtBr and after the completion of gel electrophoresis, the samples were analyzed under a UV-transilluminator.

4.5 SOD Activity

E. coli and *B. subtilis* bacterial cells were grown in fresh LB broth (1%), overnight. After this, a known concentration of bacterial cells (O.D count: 0.2), were exposed to 1 mg/ml Fenu, CuO, MnO_2, and Fe_2O_3 hydrogel samples, with the untreated cells as control and kept for incubation at 37°C, overnight. The treated cells were collected and subsequently homogenized to disrupt the cellular structure. The resulting homogenate was then subjected to centrifugation at 10000 rpm for 10 minutes, allowing for the separation and collection of the supernatant fraction. A solution containing 800 µl of (30 mM) methionine, (0.02 mM) riboflavin, (0.75 mM) NBT, (20 mM) phosphate buffer (pH 7.8) was prepared and to this, the supernatant (200 µl) was added. The reaction mixture was exposed to a fluorescent lamp for 10 mins, following which absorbance was detected at a wavelength of 560 nm. The following formula was used to calculate superoxide dismutase (SOD) activity.[6]

$$\text{SOD Activity}(\%) = \frac{\text{Abs}_{(Control)} - \text{Abs}_{(Sample)}}{\text{Abs}_{(Control)}} \times 100$$

4.6 Catalase Study

E. coli and *B. subtilis* bacterial cells were grown in fresh LB broth (1%), overnight. After this a known concentration of bacterial cells (O.D count: 0.2), were exposed to 1 mg/ml Fenu, CuO, MnO_2, and Fe_2O_3 hydrogel samples, with the untreated cells as control and kept for incubation at 37°C, overnight The treated cells were collected and subsequently homogenized to disrupt the cellular structure. The resulting homogenate was then subjected to centrifugation at 10000 rpm for 10 minutes, allowing for the separation and collection of the supernatant fraction. The supernatant was combined with 40mM H_2O_2 solution and incubated at 37°C for 10 minutes. Following this, the mixture was further mixed with Titanium Sulphate (1% w/v), which developed a yellow-colored complex, and the absorbance was measured at 405 nm. The following formula was used to calculate the H_2O_2 scavenging activity.[7]

$$\text{Catalase Activity}(\%) = \frac{\text{Abs}_{(Control)} - \text{Abs}_{(Sample)}}{\text{Abs}_{(Control)}} \times 100$$

4.7 Protein Leakage Study

The disruption of the cell membrane and subsequent leakage of cellular proteins following bacterial death was estimated by Bradford assay. Bacterial cells cultured to a known concentration (O.D: 0.2) were treated with 1mg/ml nanocomposite hydrogels, while the control had no such antibacterial agent. After overnight incubation at 37°C, 1ml from all the culture samples was subjected to centrifugation at 10000 rpm for 10 minutes for harvesting the supernatant that was further used for measuring the quantity of cellular protein through the Bradford assay by measuring the absorbance at 595 nm wavelength. A standard curve was plotted using known BSA protein concentration (1mg/ml) and the protein estimation was done following the standard.[8]

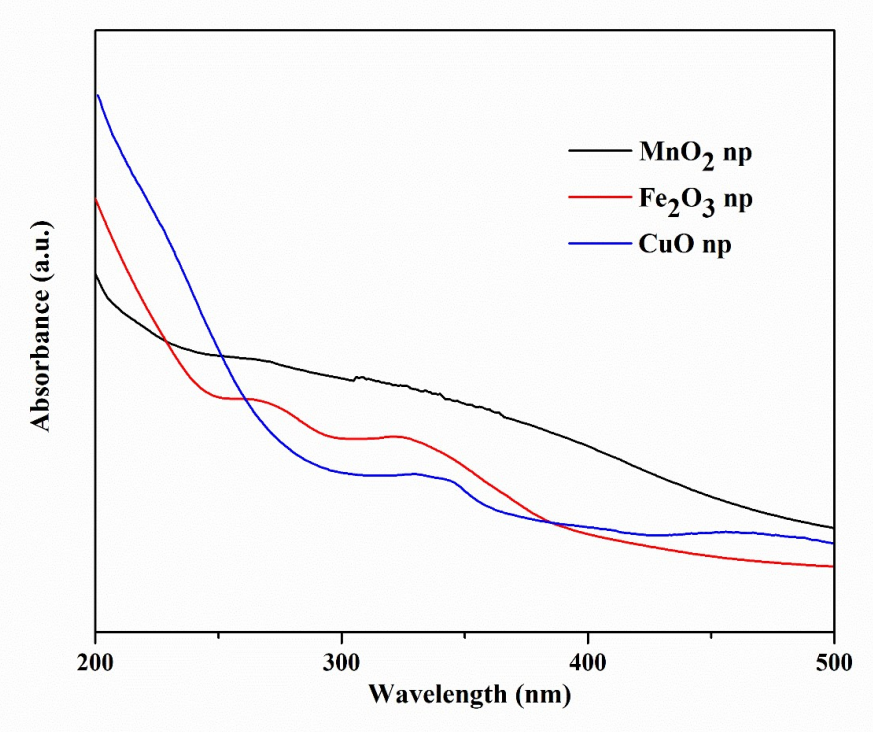

Figure S1. UV Spectra of MnO_2, Fe_2O_3, CuO nanoparticles.

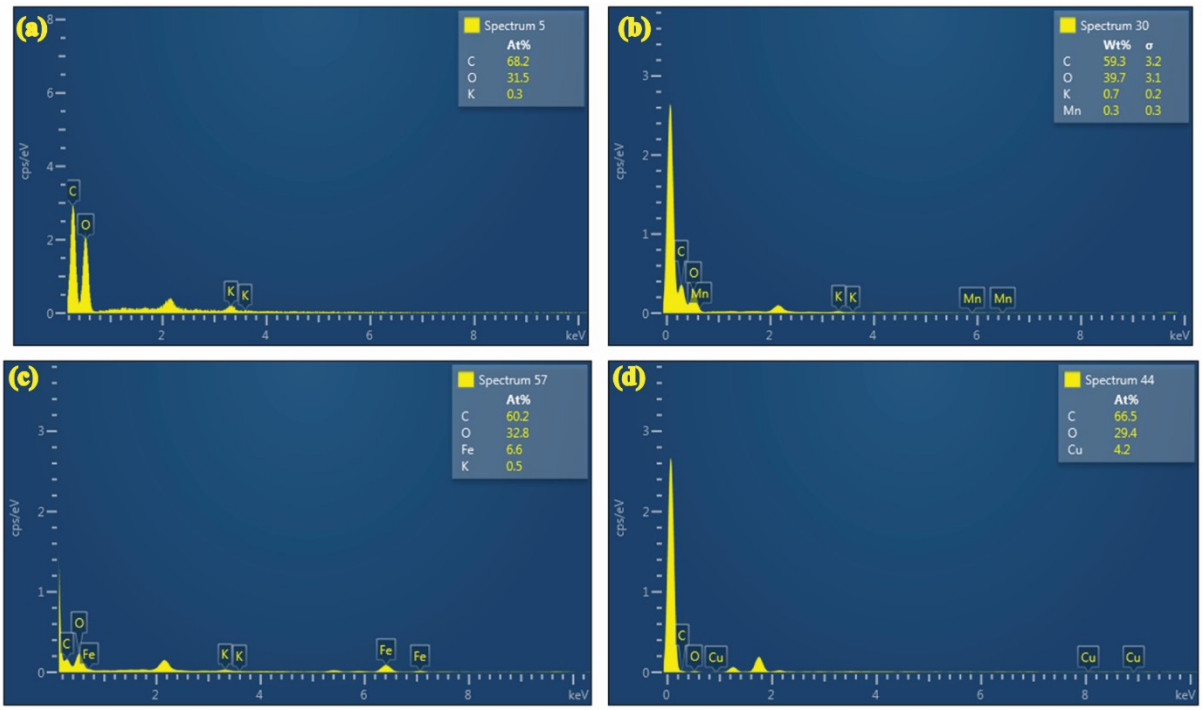

Figure S2. EDX Spectra of a) Fenu, b)MnO_2, c)Fe_2O_3, and d)CuO nanocomposite gels.

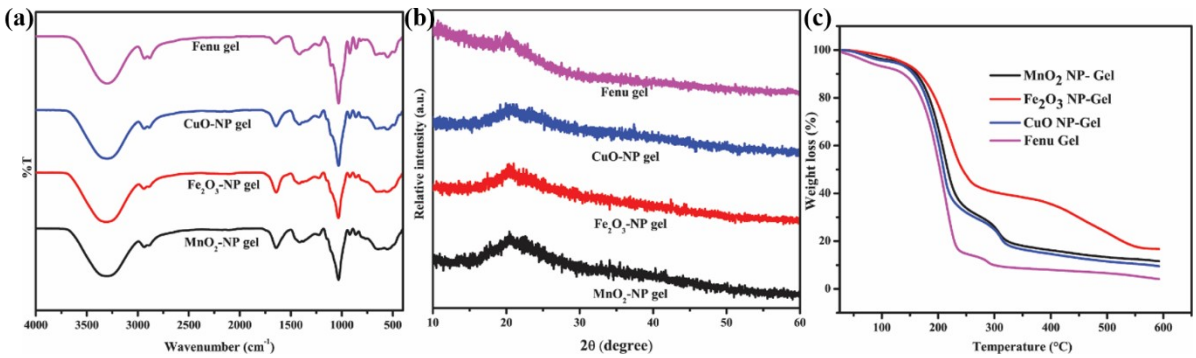

Figure S3. (a) FT-IR, (b) PXRD, and (c) TGA of Fenu, MnO_2, Fe_2O_3, and CuO nanocomposite gels.

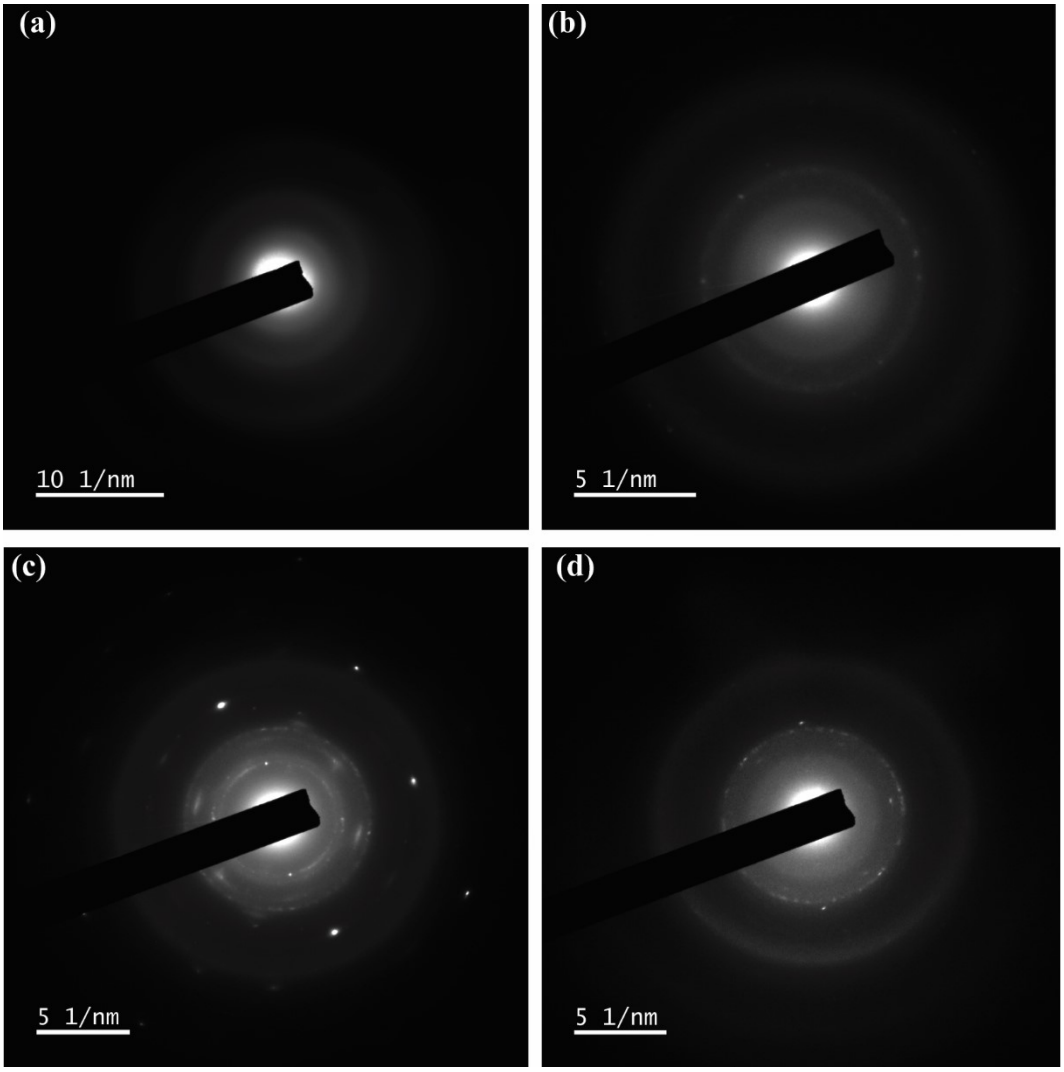

Figure S4. SAED Pattern of Fenu, MnO_2, Fe_2O_3, and CuO nanoparticles in nanocomposite gel.

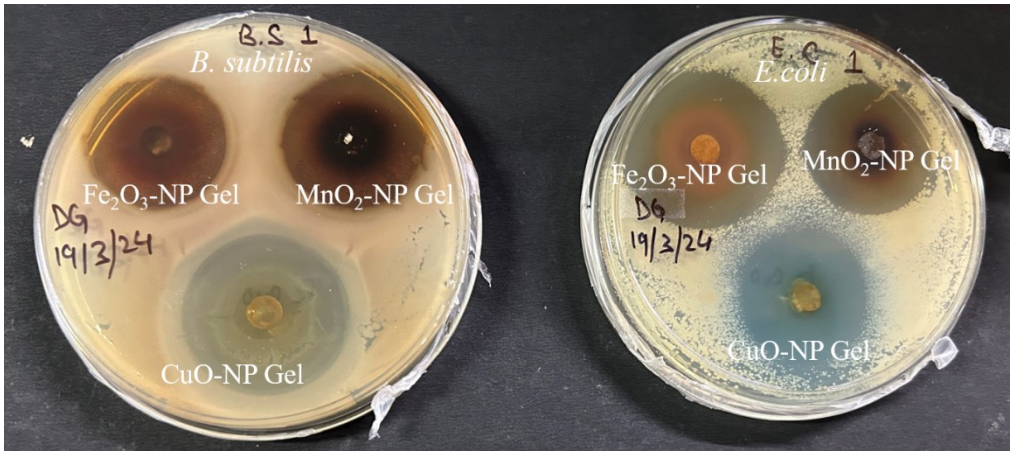

Figure S5. Zone of Inhibition studies of MnO_2, Fe_2O_3, and CuO nanocomposite hydrogels against *B.subtilis* and *E.coli* bacteria.

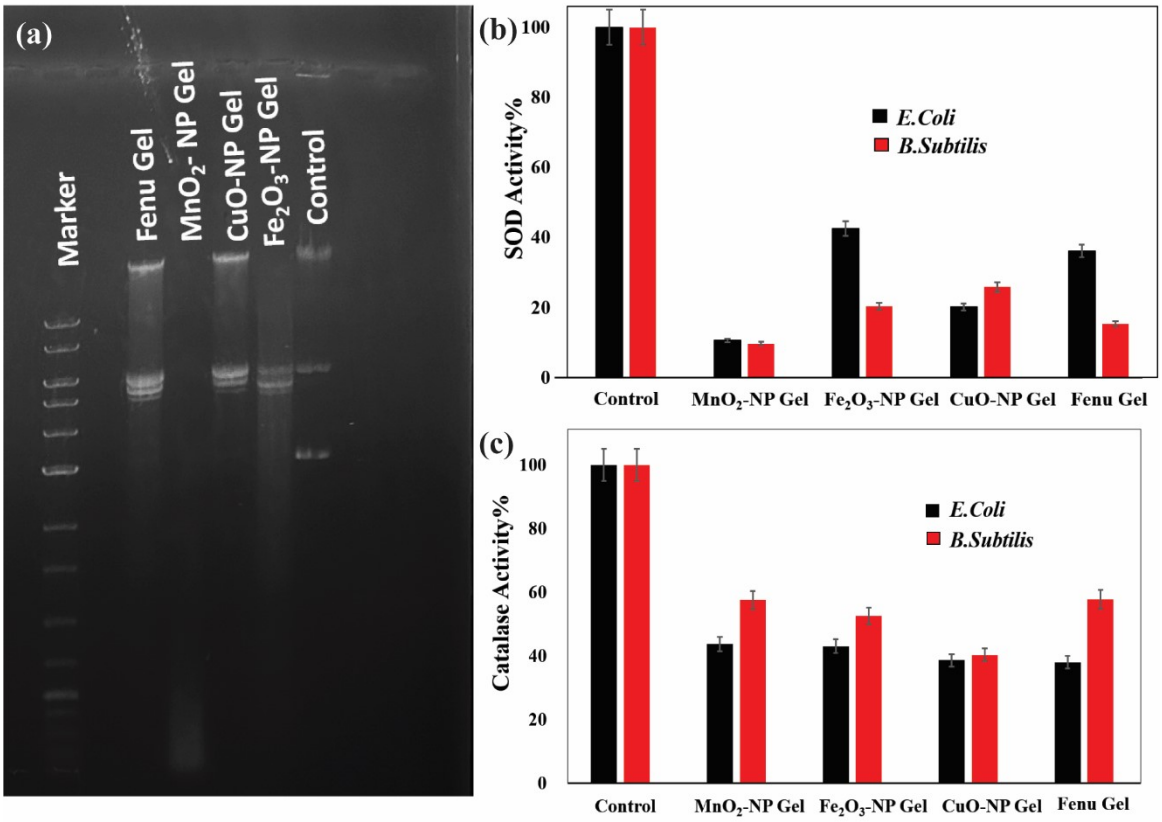

Figure S6. a) DNA Fragmentation studies of pET-28a plasmid using MnO_2, Fe_2O_3, CuO, and Fenu nanocomposite hydrogels b) SOD Activity % and c) Catalase Activity % studies of MnO_2, Fe_2O_3, CuO and Fenu nanocomposite hydrogel- treated *B.subtilis* and *E.coli* bacteria.

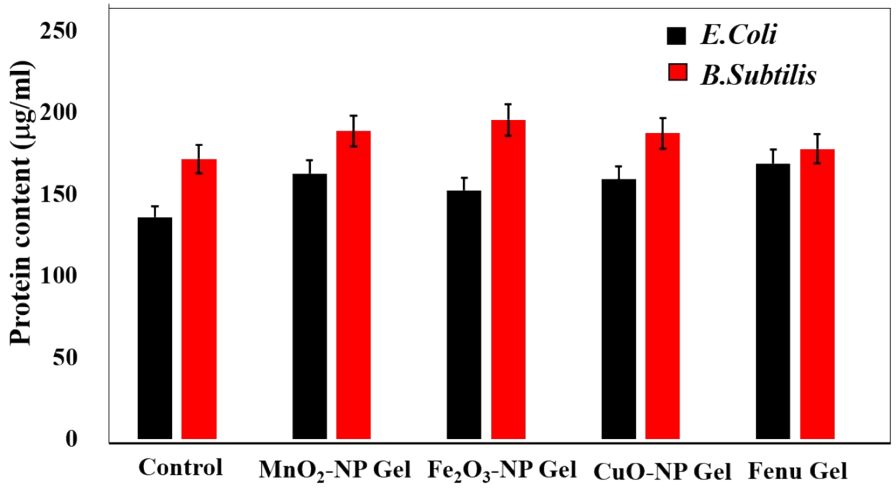

Figure S7. Protein Leakage studies of MnO_2, Fe_2O_3, CuO, and Fenu nanocomposite hydrogel-treated *B.subtilis* and *E.coli* bacteria.

Table S1 : Some literature survey on antibacterial mechanism of action of nanocomposites

Sl. No	Type of Nanocomposites	Mechanism of Action	Effectiveness	Factors	References
1.	ZnO	Cell membrane damage, Higher photocatalytic activity, ROS Generation, Zinc Ion release, Disruption of electron transport membrane	Both Gram-positive and Gram-negative bacteria	Size and Shape	[9-12]
2.	TiO_2	ROS generation, lipid peroxidation, electrostatic interation with cell membrane, inhibit quorum sensing	Gram positive and Gram-negative bacteria	Structure, Size and Shape	[13-16]
3.	MgO	Cell membrane damage	Both Gram-positive and Gram-negative bacteria	Size, Shape, Aggregation	[17-18]
4.	MnO_2	ROS generation, disruption of antioxidant defence	Gram-positive bacteria	Size, Shape,Crystal Structure	[19-21]

		enzymes, membrane damage	(major) and gram-negative bacteria		
5.	Fe_2O_3	Photocatalysis, Fenton Reaction, ROS generation, Membrane damage	Both Gram-positive and Gram-negative bacteria	Size, Shape,Surface Charge, Crystallinity	[22-24]
6.	CuO	Lipid Peroxidation, Cell leakage, Enzyme disruption, protein inactivation, DNA damage	Both Gram positive and Gram-negative bacteria	Size, Shape	[25-27]

REFERENCES

1. D. Ghosh and G. Das, *New J. Chem.*, 2024, **48**, 14049-14055.
2. D. Ghosh, M. Basak, D. Deka and G. Das, *Int. J. Biol. Macromol.*, 2023, **229**, 615-623.
3. J. Yoonus, R. Resmi and B. Beena, *Mater. Today: Proc.*, 2021, **46**, 2969-2974.
4. S. Goswami, D. Thiyagarajan, G. Das, and A. Ramesh, *ACS Appl. Mater. Interfaces*, **6**, 16384-16394.
5. S.Ehrt, and D. Schnappinger, *E. coli Plasmid Vectors: Methods and Applications*, 2003, 75-78.
6. K.S. Sivasuriyan, S.K.R. Namasivayam, and A. Pandian, *Int. J. Biol. Macromol.,* 2025, **286**, 138495.
7. M. Rajkumar, S.D. Presley, P. Govindaraj, D.Kirubakaran, F. Farahim, T Ali, M. Shkir, and S. *Sci. Rep.*, 2025, **15**(1), 3931.
8. P.S. Ju, H.Z. Mei, Z.L. Jia, J.J. Fu, M.L. Jun, L.D. Tong, H.X. Song and C. Fang, *J. Drug Deliv.Sci.Technol.* 2024, **100**, 105951.
9. T.A.Singh, A. Sharma, N. Tejwan, N.Ghosh, J. Das, and P.C. Sil, *Adv. Coll.Int. Sci.*, 2021, **295,** 102495.
10. C.Pushpalatha, J. Suresh, V.S. Gayathri, S.V. Sowmya, D. Augustine, A. Alamoudi, B. Zidane,N.H. Mohd. Albar and S. Patil, *Front.bioeng. biotechnol.,2*022, **10**, 917990.

11. A.A. Alswat, M.B. Ahmad, T.A. Saleh, M.Z.B. Hussein, and N.A. Ibrahim, *Mater. Sci. Eng.: C*, 2016, **68**, 505-511.
12. M.Y. Al-darwesh, S.S. Ibrahim, M.A. Mohammed, *Results chem.*, 2024,**7**, 101368.
13. V.Saisruthi, J.A. Kumar, N.T.M. Rosana, K.L.V. Joseph, and S.J. Rubavathy,2024,**34**, e22359.
14. B.Zhou, X.Zhao, and Y. Liu, *J.Text.Inst.*, 2024, 1-27.
15. D.R.Eddy, D. Rahmawati, M.D., Permana, T. Takei, A.R. Noviyanti, and I. Rahayu, I. *Inorg. Chem. Commun.*, 2024,112531.
16. Mahfooz-ur-Rehman, W.Rehman, M. Waseem, B.A. Shah, M. Shakeel, S. Haq, U. Zaman, I.Bibi and D.H. Khan, *J. Chem.Eng. Data*, 2019, **64**, 2436-2444.
17. Y.H. Leung, A.M. Ng, X. Xu, Z. Shen, L.A. Gethings, M.T. Wong, C.M. Chan, M.Y. Guo, Y.H. Ng, A.B. Djursisic and F.C. Leung, F. C. *Small*, 2014,**10**, 1171-1183.
18. A.Nigam, S. Saini, A.K. Rai, and S.J.Pawar, *Ceram.Int.*, 2021, **47,** 19515-19525.
19. H.Lu, X. Zhang, S.A. Khan, W. Li, and L. Wan, L. *Front. Microbiol.*, 2021, **12**, 761084.
20. M.F.Warsi, K.Chaudhary, S. Zulfiqar, A. Rahman, I.A. Al Safari, H.M. Zeeshan, P.O. Agboola, M. Shahid, and M. Suleman, *Ceram. Int.*, 2022, **48**, 4930-4939.
21. S.Elbasuney, A.M. El-Khawaga, M.A. Elsayed, A. Elsaidy, M. Yehia, and M.A. Correa-Duarte, *Sci. Rep.*, 2024,**14**, 15658.
22. S.V.Gudkov, D.E. Burmistrov, D. A. Serov, M.B.Rebezov, A.A. Semenova, and A.B. Lisitsyn, Do iron oxide nanoparticles have significant antibacterial properties?. *Antibiotics*, 2021, **10**, 884.
23. H.J.Fatih, M. Ashengroph, A.Sharifi, and M.M. Zorab, *BMC microbiol.*,2024, **24,** 535.
24. M.Bhushan, D. Mohapatra, Y. Kumar, A.K. Viswanath,*Mater. Sci.Eng.: B*, 2021,**268**, 115119.
25. G.Applerot, J. Lellouche, A. Lipovsky, Y. Nitzan, R. Lubart, A. Gedanken, and E. Banin, *Small*, 2021**, 8(21),** 3326-3337.
26. P.Nisar, N. Ali, L. Rahman,M. Ali, and Z.K. Shinwari, *JBIC J. Biol. Inorg.Chem.*, 2019,**24,** 929-941.
27. I.Perelshtein, G.Applerot, N. Perkas, E. Wehrschuetz-Sigl, A. Hasmann, G. Gübitz, and A. Gedanken, *Surf.Coat.Technol.*, 2009, **204,** 54-57.